The Astrophysical Journal Letters, 991:L26 (6pp), 2025 September 20 https://doi.org/10.3847/2041-8213/ae04e3

Which Solar Latitude Follows the Sunspot Cycle Exactly?

K. P. Raju
Indian Institute of Astrophysics, Bangalore 560034, India
Received 2025 March 17; revised 2025 September 4; accepted 2025 September 5; published 2025 September 19

Abstract

The large-scale convection in the Sun known as supergranulation is manifested as a network structure on the solar surface. The network cells have an average lifetime of 24 hr, a size of about 30 Mm, and a lane width of about 6 Mm. We have obtained the lane widths and intensities at different latitudes from the Ca II K spectroheliograms from the 100 yr Kodaikanal archival data. We have then calculated the cross-correlation function of lane widths and intensities with sunspot number at every latitude from 60°N to 60°S. The correlation coefficients of the quantities show an approximate north–south symmetry with broad peaks around $\pm(11–22)^\circ$ latitude with values of about 0.8. The results imply that these latitudes follow the sunspot cycle strongly. The maximum correlation for the lane widths occurs $(18 \pm 2)^\circ$N and $(20 \pm 2)^\circ$S with no phase difference. For intensities, this happens at $(13 \pm 2)^\circ$N and $(14 \pm 2)^\circ$S with a phase difference of 1.25–1.5 yr. It is interesting to note that the lane width correlations peak during the solar maximum, whereas the intensity correlations peak 1.25–1.5 yr after the solar maximum. The results generally show that no unique latitude exactly follows the solar cycle for all quantities. The results are important in flux transport on the solar surface and have implications for the quiet Sun UV irradiance variations.

Unified Astronomy Thesaurus concepts: Solar cycle (1487); Solar atmosphere (1477)

1. Introduction

The two basic scales of solar convection are granulation and supergranulation. Granulation is the small scale and the supergranulation is the large scale, which is manifested as a network structure on the solar surface. The network cells have an average lifetime of 24 hr, a size of about 30 Mm, and a lane width of about 6 Mm. The network arises due to magnetic flux concentration at cell boundaries as a consequence of supergranular convection (R. B. Leighton et al. 1962; G. W. Simon & R. B. Leighton 1964). Skylab observations in the 1970s have shown that the chromospheric network extends to the transition region as the EUV network (E. M. Reeves 1976). The network is dominant in the midtransition region, and it disintegrates in the corona (P. T. Gallagher et al. 1998). Several interesting findings in recent years have raised questions on the origin of supergranulation and why it occurs primarily at about the 30 Mm scale. The original suggestion by G. W. Simon & R. B. Leighton (1964) that the helium recombination plays a role in forming the supergranular scales is not supported by simulations or models (J. W. Lord et al. 2014; H. Hotta et al. 2023). A thermal convective origin of supergranulation has long been the credible explanation, but the contribution of other factors like rotation, magnetic field, and multiscale convection is also being considered (F. Rincon & M. Rieutord 2018). T. L. Duvall (1980) and H. B. Snodgrass & R. K. Ulrich (1990) found that supergranulation rotates faster than the surrounding plasma, which is referred to as superrotation. L. Gizon et al. (2003) found that the supergranulation pattern had wavelike properties with a typical period of 6–9 days, much longer than the individual supergranules' lifetime. L. Gizon et al. (2010) use local helioseismology to show the effect of the Coriolis force on supergranular flows. T. Roudier et al. (2014) reported that supergranular motions reflect solar differential rotation and a poleward meridional flow. Also, the presence of magnetic fields was found to weaken diverging flows. J.-F. Cossette & M. P. Rast (2016) suggest that the supergranular scale is the largest buoyantly driven mode of convection in the Sun. A. V. Getling & A. G. Kosovichev (2022) found that the horizontal flow scales increase rapidly with depth. The total power of the convective flows is anticorrelated with the sunspot number variation in subsurface layers and positively correlated at larger depths. C. S. Hanson et al. (2024) analyzed Dopplergrams from the Solar Dynamics Observatory to identify 23,000 supergranules. They found that the vertical flows peak at a depth of 10,000 km, and the supergranular convection is not explained by mixing-length theory.

Solar activity levels may influence supergranulation properties such as its scale, lifetime, and flow velocity (N. Meunier et al. 2007, 2008). The dependence of supergranular size on the solar cycle has remained controversial. A decrease of cell sizes has been reported by J. Singh & M. K. V. Bappu (1981), F. Berrilli et al. (1999), K. P. Raju & J. Singh (2002), R. Kariyappa & K. R. Sivaraman (1994), M. L. De Rosa & J. Toomre (2004), and C. Huang et al. (2012), but H. Wang (1988), H. Muenzer et al. (1989), and N. Meunier (2003) pointed out an increase of network cell sizes. N. Meunier et al. (2007) suggest that a negative or a positive correlation can be obtained, depending on whether the level of magnetic activity is defined with respect to internetwork or network fields. S. W. McIntosh et al. (2011) found a reduction of 0.5 Mm in the average supergranular radius during the cycle 23/24 minimum compared to the cycle 22/23 minimum. S. Mandal et al. (2017) found that mean scale values are highly correlated with the sunspot cycle amplitude. S. Chatterjee et al. (2017) showed that the active region supergranule mean scale varies in phase with the solar cycle, whereas for the quiet region supergranule mean scale, it is the opposite.

In addition to the size, there is another length scale associated with the supergranulation: the lane width. In their seminal work, G. W. Simon & R. B. Leighton (1964) obtained the lane width through a manual autocorrelation method and interpreted it as a measure of magnetic flux at the supergranular cell boundaries. Although the lane width and size show some similarities in their behavior (J. Sýkora 1970; C. Gontikakis et al. 2003), their interrelationship and the possible role of lane width in supergranular origin are not known. However, several interesting results have been obtained from lane width studies. J. Sýkora (1970) reported asymmetry in the supergranular length scales from Ca K spectroheliogram measurements. Both lane widths and sizes were found to be lengthened in the direction of the solar rotation. The lane widths were found to have an almost constant width up to the upper transition region and then fan out rapidly at coronal temperature, which supports the funnel model of the network magnetic field (S. Patsourakos et al. 1999). C. Gontikakis et al. (2003) found that the size and lane widths generally increase with the formation temperatures of the chromospheric and transition region emission lines. From Solar and Heliospheric Observatory (SOHO)/Solar Ultraviolet Measurement of Emitted Radiation data, H. Tian et al. (2008) found that the network lane width is smaller in the chromosphere than in the transition region. In an earlier work (K. P. Raju 2016), we have obtained the network lane width from the SOHO/Coronal Diagnostic Spectrometer (CDS) synoptic images of the Sun in He I 586 Å and O V 630 Å. The lane widths are found to be correlated with the solar cycle variation with a lag of about 10 months. The data also show large asymmetry in network lane widths in the horizontal and vertical directions caused by image distortions in the CDS due to instrumental effects. We have also obtained the network lane widths and intensities from the Ca II K spectroheliograms from the Kodaikanal archival data (K. P. Raju 2018). The results show that both quantities are dependent on the solar cycle. Also, a varying phase difference between the quantities has been noticed in different solar latitudes, and evidence of equatorward flux transfer. It is also found that the lane widths, obtained near the midlatitudes during the sunspot cycle minima, are strongly correlated to the following sunspot number maxima. The strong correlation of the two parameters provides a simple way to predict the maximum sunspot number about 4–5 yr in advance (K. P. Raju et al. 2023).

As the previous paragraph shows, the lane width and intensities depend on the solar cycle. The lane width from SOHO/CDS EUV images shows a time lag of about 10 months in the equatorial region. In the present Letter, we examine the relationship between the solar cycle and two physical quantities, lane widths and intensities, in more detail. We would like to see how the time lag between the quantities varies in different latitudes. We want to examine the cross correlation between these quantities and see where the correlation coefficient reaches a maximum. We examine all latitudes from 60°N to 60°S to see whether any particular latitude follows the solar cycle exactly. We use the newly calibrated Kodaikanal archival data (M. Priyal et al. 2014) in the study. The following sections describe the details of the data analysis, results, and conclusions.

2. Data and Analysis

The present analysis uses about 34,000 Ca II K spectroheliograms from the Kodaikanal Solar Observatory. The instrument used is the same throughout the 100 yr of observation. It is a spectroheliograph where no filter is involved. The exit slit is centered at the Ca K line at 3933.67 Å with a spectral window of 0.5 Å. The centering of the Ca K line has a maximum uncertainty of about 0.1 Å due to the visual setting of the spectrum and due to the stability of the spectroheliograph (M. Priyal et al. 2014). This affects the contrast of the spectroheliograms. There are also other factors affecting the contrast, such as change of photographic emulsions, development, sky transparency, and variations in density-to-intensity conversion. The contrast changes are effectively corrected using the "equal-contrast technique" (J. Singh et al. 2021). The images are corrected for limb darkening, and their contrast is adjusted until the FWHM of the intensity distribution attains a value between 0.10 and 0.11. The resulting intensity is normalized with values varying from 1.0 to 1.1 for the quiet Sun, 1.1–1.2 for the active network, and >1.2 for active region plages. The spatial resolution of the data is about 2″ (M. K. V. Bappu 1967). The data are obtained from 1907 to 2007, but we have considered images only until 1990 as there was a seeing deterioration after this time (R. Sridharan 2017-18). The details of the data analysis are described in K. P. Raju (2020). The image windows of size 120 arcsec^2 containing about 16 supergranules are taken from the central meridian in the latitude range 60°N to 60°S with an interval of 1°. The window sizes are corrected for foreshortening effects on the solar surface. Active region windows are avoided by applying the following intensity criterion. Based on the mean intensity of the windows, we rejected those at the top and bottom 5% of the distribution (K. P. Raju et al. 2023). This removes the low-exposure regions at the lower end and the active regions and active network at the higher end. The threshold is decided through a trial and error method. Varying the threshold by a few percent does not significantly affect the correlation. Lane width is measured as the width of the autocorrelation function (K. P. Raju et al. 2023) of the image window. Lane widths and the mean intensity are obtained for every image window, and the annual variations are removed by averaging them over a year. The corrected lane widths and intensities are obtained as functions of latitude and time.

3. Results

We obtained the temporal variations of lane widths and intensities averaged over a year in the latitude range 60°N to 60°S with an interval of 1°. The variation is plotted in Figure 1 for 13 representative latitudes. The yearly averaged sunspot number variation is also shown. It is found that the latitudes near ±20° have the solar cycle modulations. The lane width data generally have more prominent modulations than the intensity data. The solar cycle variation of Ca K intensity is up to 5%.

Next, the cross correlation of lane width and intensity with sunspot cycle as a function of lag (year) is obtained at the different latitudes. This is shown in Figure 2. As in Figure 1, the correlation of lane width and intensity with sunspot cycle is very high in the latitudes near ±(11–22)°. The maximum correlation coefficient is about 0.8, and it decreases toward higher and lower latitudes. At 60°N and also at the equator, the lane width and intensity correlation curves are nearly in opposite phases with each other, although with reduced correlation coefficients. Similar anticorrelations are reported in the polar activity indices by M. Priyal et al. (2023). A closer examination of latitudes shows significant differences in the behavior of lane widths and intensities. This is shown in the

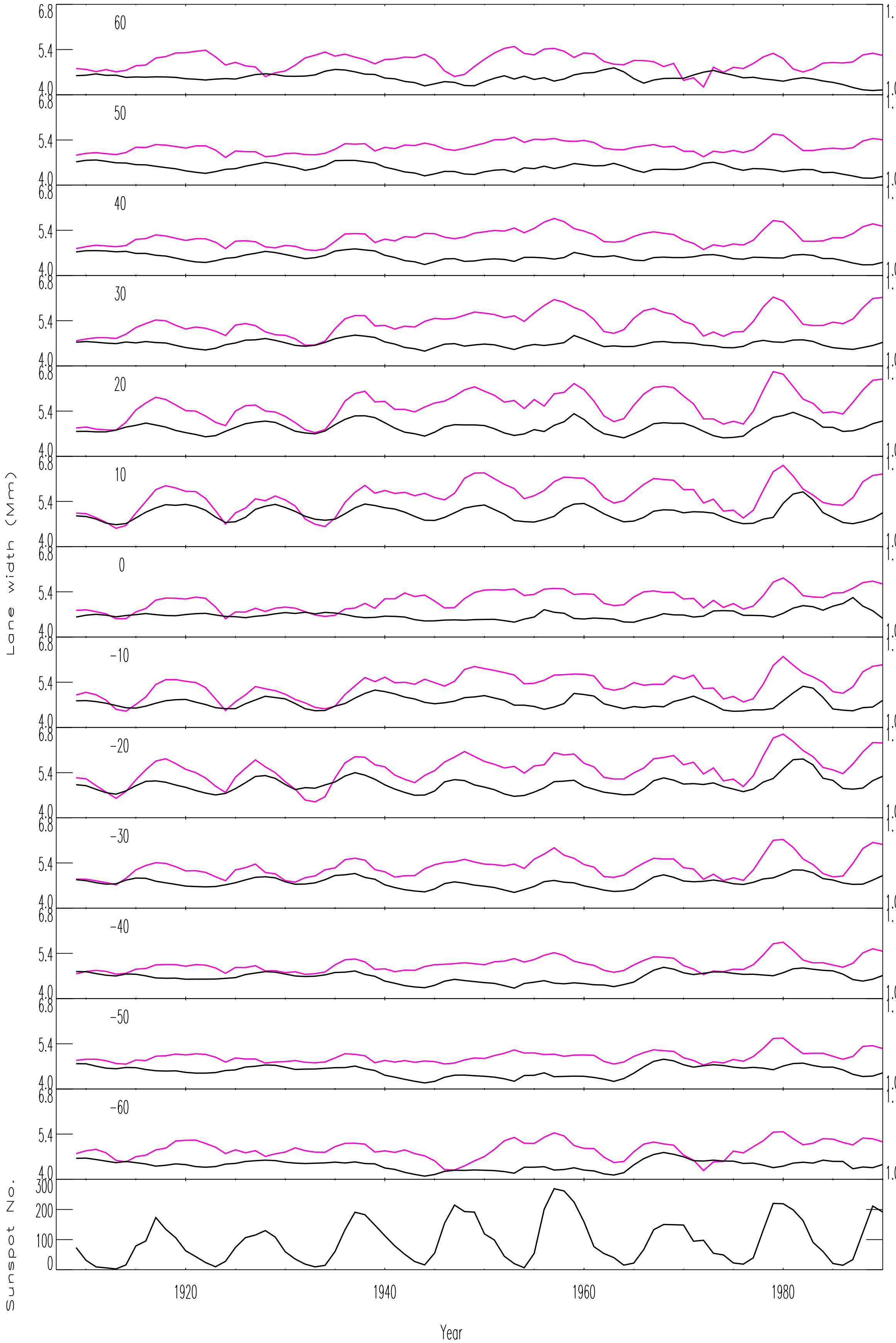

Figure 1. Yearly averaged supergranular lane widths (pink) and Ca K intensity (black) as a function of time for different latitudes from 60°N to 60°S with an interval of 10°. The *y*-axis on the right gives the normalized intensity. The bottom panel shows the variation of the yearly averaged sunspot number with time. Sunspot data from the World Data Center SILSO, Royal Observatory of Belgium, Brussels.

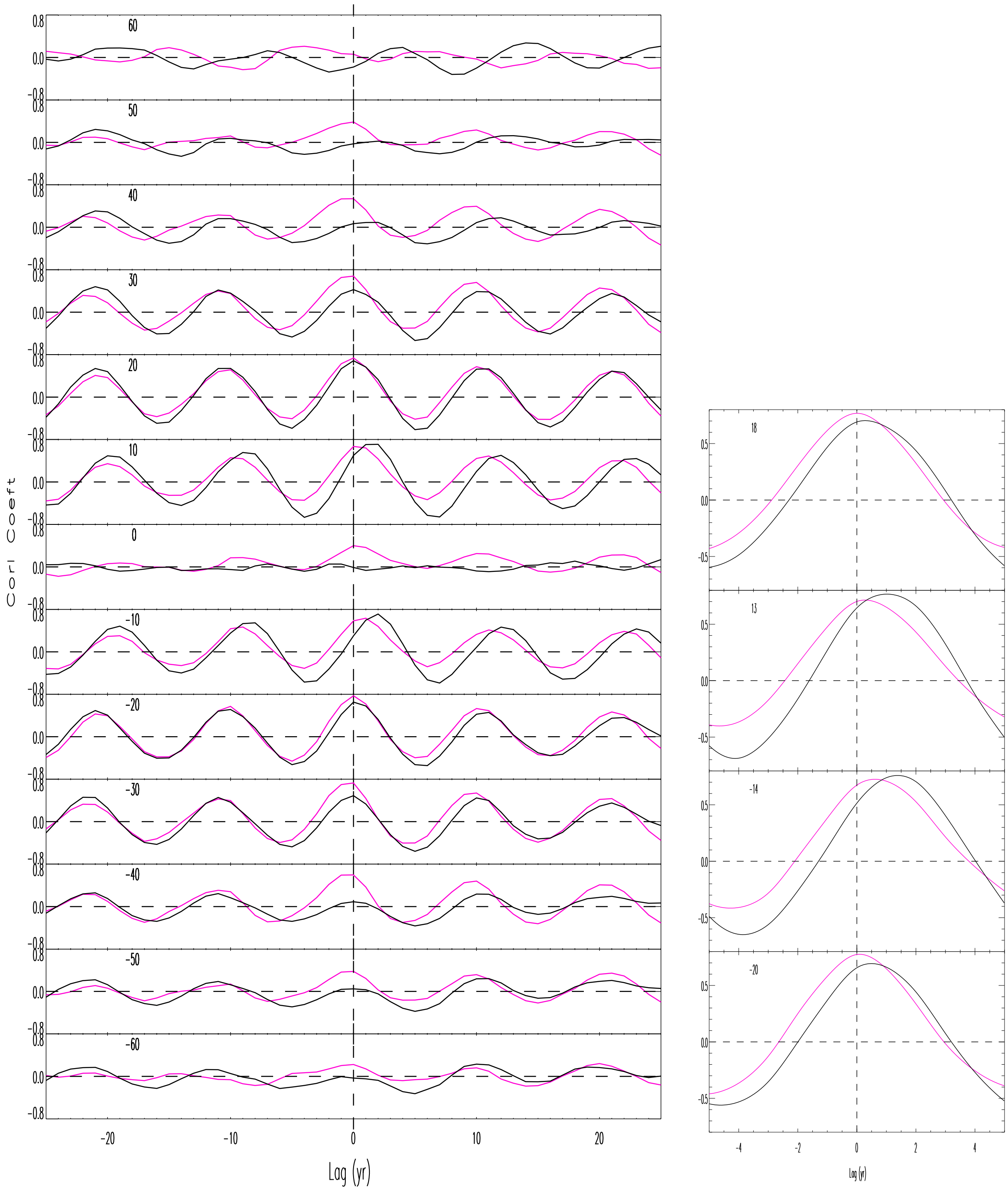

Figure 2. Cross correlation of lane widths (pink) and intensities (black) with sunspot cycle as a function of lag (year) at different latitudes. The panels on the right give a magnified view of the central region ($-5 < \text{lag} < 5$) at selected latitudes.

right panels of Figure 2. The maximum correlation for the lane widths occurs at 18°N and 20°S with no phase lag. For intensities, this happens at 13°N and 14°S with a phase lag of 1.25–1.5 yr. The results imply that there is no unique latitude that follows the sunspot cycle; the intensity and lane width follow the sunspot cycle in slightly different ways.

It can also be noted that there is a systematic change in the lag in latitudes. For both lane widths and intensities, the lag is zero near ±20°, which decreases toward higher latitudes and increases toward the equator. There is a difference in the magnitude of lag for lane width and intensity with the sunspot cycle. This aspect is studied in more detail in the following.

Note that the *x*-axis interval is 1 yr. We aim to get the exact time lag corresponding to the maximum correlation coefficient within the fraction of a year. For this, we took the data from Figure 2 in the range ±5 yr (close to one solar cycle) and interpolated it with an interval of 0.01 yr. The maximum correlation coefficient of lane width and intensity with sunspot cycle at different latitudes is plotted in the top panel of Figure 3. A five-point smoothing average is also plotted, which shows the peaks somewhat better. The peaks are still broader but can be specified with an uncertainty of ±2°. It can be seen that the plots are nearly symmetrical with respect to the equator, but there are notable deviations from symmetry. The

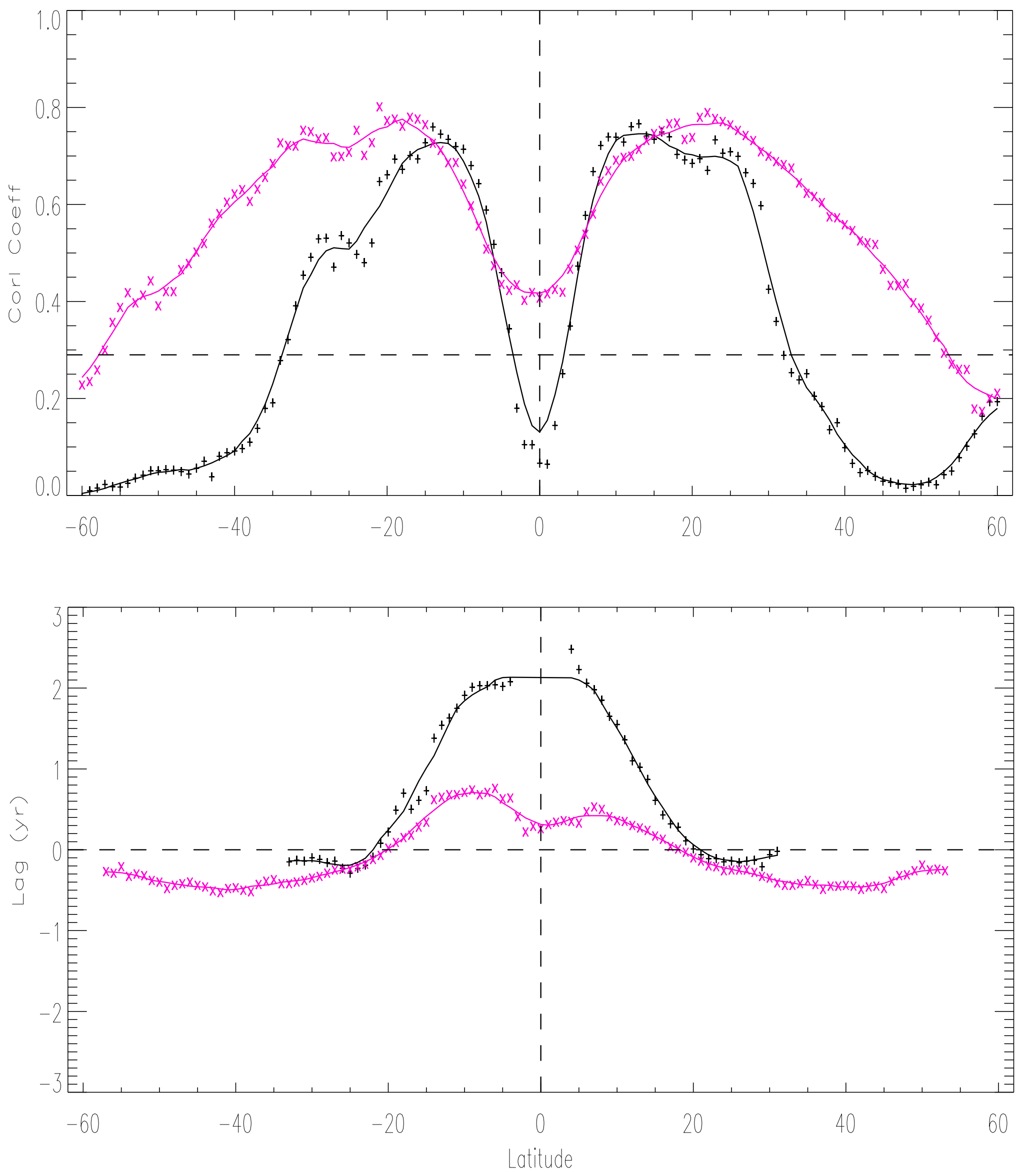

Figure 3. Maximum correlation coefficient of lane width (pink) and intensity (black) with sunspot cycle at different latitudes (top). The continuous line represents a five-point smoothing average. The horizontal dashed line represents the 99% confidence level. Lag (year) of lane width (pink) and intensity (black) with solar cycle at different latitudes (bottom). Only those points with a correlation coefficient above 0.29 (99% confidence level) are shown.

peaks are closer to the equator in the north. The multiple components are seen at lower levels in the north. There is also a sharp turnaround in the intensity correlations beyond 50°N, although with reduced significance. For lane width, the correlation coefficient is 0.45 at the equator, 0.8 near ±20°, and about 0.2 near ±60°. For intensity, the correlation coefficient is close to zero at the equator, 0.8 near ±13°, and close to zero near ±50°. The correlation coefficients show a multicomponent structure in both hemispheres. There is a marked phase lag between the lane width and intensity plots; intensity reaches the maximum correlation in much lower latitudes in the two hemispheres. At the level of the correlation coefficient = 0.5, the width of the lane width peaks is about 40°, whereas the width of the intensity peaks is 20°.

The bottom panel shows the lag (year) of lane width and intensity with solar cycle at different latitudes. Only those points with a correlation coefficient above 0.29—highly significant correlation where the probability of occurrence by chance is less than 1%—are shown. The plots are nearly symmetric here too. The lag varies from −0.5 to 0.8 yr for lane width. For intensity, the lag varies from −0.3 to about 2.5 yr. Also, note that there is a broad reversal in the lag values for both quantities; at about ±(25 ± 2)° for intensity and ±(40 ± 2)° for lane width.

It may be noted that the autocorrelation function from Ca K image windows gives two length scales of supergranulation; namely, the lane width and the size (K. P. Raju et al. 2023). Our results indicate a highly significant correlation between lane width and sunspot cycle in the latitude range 55°S–55°N. The relationship between lane width and size is not clear now. So, the current work may not resolve the conflicting reports on the cycle dependency of the size, but it may give some useful, related information.

It is interesting to note that the intensities and the lane widths behave in different ways at different latitudes. We know that both lane widths and intensities are dependent on local magnetic flux, so there could be other factors that may influence their behavior. Lane width is a measure of magnetic flux at the supergranular cell boundaries (G. W. Simon & R. B. Leighton 1964). Intensity, on the other hand, also depends on the temperature and chemical abundance. Measurements of sunspots over the solar latitudes show a peak around ±13°–15°. (R. F. Howard 1994). This is consistent with our results, which show that the intensity peaks at (13 ± 2)°N and (14 ± 2)°S. For lane width, the peaks appear after about 5°. Magnetic flux is mainly transported on the solar surface by differential rotation, granular and supergranular convection, and meridional flows. G. Sindhuja et al. (2014) find evidence of meridional flow from their Ca II K line profile analysis. The study needs to be continued with more data sets to ascertain the reasons for the behavior of the two quantities, which may bring out interesting aspects of flux transport on the solar surface.

4. Conclusions

We conducted an extensive analysis of the newly calibrated Ca II K spectroheliograms from Kodaikanal archival data and obtained the intensities and supergranular lane widths as functions of latitude and time. We obtained the cross-correlation function of these quantities with the sunspot cycle to see the variation of correlation coefficients as a function of time lag at each latitude within the range 60°N–60°S with an interval of 1°. The following major points can be noted.

1. The main aim is to see whether any particular latitude follows the solar cycle exactly. The maximum correlation for the lane widths occurs at (18 ± 2)°N and (20 ± 2)°S. For intensities, this happens at (13 ± 2)°N and (14 ± 2)°. The results generally show that no unique latitude exactly follows the solar cycle for all quantities. For different physical quantities, the correlation reaches a maximum at different latitudes.

2. The above finding on maximum correlation is comparable to the results of R. F. Howard (1994), who reports that sunspot distribution over the solar latitudes peaks around ±13°–15°. There is a good agreement for intensity, whereas there is a difference of about 5° for lane width.

3. The total solar irradiance depends on the sunspot cycle, and the amplitude of variation is about 0.1% from minimum to maximum (T. Chatzistergos et al. 2023). However, the variation of UV irradiance is more than an order of magnitude, about 1.5% (J. Lean 1989). For individual spectral lines, the variation can be even more. Our results show that the solar cycle variation of Ca K intensity is up to 5%.

4. Another interesting finding is that the lane width correlations peak during the solar maximum, while the intensity correlations peak 1.25–1.5 yr after the solar maximum.

5. The correlation coefficients of both quantities show an approximate north–south symmetry. The results show that for lane width, the correlation is significant in a broad range (about 55°N–55°S), whereas for intensity, the range is much narrower (about 5°–35°N and 5°–35°S). The lack of significant correlation for quiet Sun Ca K intensity at the solar equatorial region is unexpected.

6. Another important difference between lane width and intensity behavior is in the time lag. The lag varies from −0.5 to 0.8 yr for lane width; for intensity, it varies from −0.3 to about 2.5 yr. The reason for this significant difference is not apparent.

7. The current work may not resolve the controversy of the cycle dependency of the supergranular size. Still, it can be concluded that the supergranular lane width depends on the solar cycle for the quiet Sun. A highly significant positive correlation is found in the latitude range 55°S–55°N.

Supergranular diffusion is one of the ways by which magnetic flux is transported on the solar surface. The phase lag between lane width and solar cycle is due to the flux transport, and its speed can be estimated. The speed of flux transport plays a vital role in the length of the solar cycle. Some of the above points (3, 4, and 5) are important to the quiet Sun UV irradiance variations. The implications of the results for the origin of supergranulation are to be understood through future studies.

Acknowledgments

This work is funded by the Department of Science and Technology, Government of India. We thank the numerous observers and the digitization team of Kodaikanal Solar Observatory for the availability of the data.

ORCID iDs

K. P. Raju https://orcid.org/0000-0002-6648-4170

References

Bappu, M. K. V. 1967, SoPh, 1, 151
Berrilli, F., Ermolli, I., Florio, A., et al. 1999, A&A, 344, 965
Chatterjee, S., Mandal, S., & Banerjee, D. 2017, ApJ, 841, 70
Chatzistergos, T., Krivova, N. A., & Yeo, K. L. 2023, JASTP, 252, 106150
Cossette, J.-F., & Rast, M. P. 2016, ApJL, 829, L17
De Rosa, M. L., & Toomre, J. 2004, ApJ, 616, 1242
Duvall, T. L. 1980, SoPh, 66, 213
Gallagher, P. T., Phillips, K. J. H., Harra-Murnion, L. K., & Keenan, F. P. 1998, A&A, 335, 733
Getling, A. V., & Kosovichev, A. G. 2022, ApJ, 937, 41
Gizon, L., Birch, A. C., & Spruit, H. C. 2010, ARA&A, 48, 289
Gizon, L., Duvall, T. L., & Schou, J. 2003, Natur, 421, 43
Gontikakis, C., Peter, H., & Dara, H. C. 2003, A&A, 408, 743
Hotta, H., Bekki, Y., Gizon, L., et al. 2023, SSRv, 219, 77
Huang, C., Yan, Y., Zhang, Y., et al. 2012, ApJ, 759, 106
Hanson, C. S., Bharati Das, S., Mani, P., et al. 2024, NatAs, 8, 1088
Howard, R. F. 1994, in ASP Conf. Ser. 14, Solar Active Region Evolution: Comparing Models with Observations Vol. 68, ed. K. S. Balasubramaniam & George W. Simon (San Francisco, CA: ASP), 1
Kariyappa, R., & Sivaraman, K. R. 1994, SoPh, 152, 139
Lean, J. 1989, Sci, 244, 197
Leighton, R. B., Noyes, R. W., & Simon, G. W. 1962, ApJ, 135, 474
Lord, J. W., Cameron, R. H., Rast, M. P., et al. 2014, ApJ, 793, 24
Mandal, S., Chatterjee, S., & Banerjee, D. 2017, ApJ, 844, 24
McIntosh, S. W., Leamon, R. J., Hock, R. A., et al. 2011, ApJL, 730, L3
Meunier, N. 2003, A&A, 405, 1107
Meunier, N., Roudier, T., & Rieutord, M. 2008, A&A, 488, 1109
Meunier, N., Roudier, T., & Tkaczuk, R. 2007, A&A, 466, 1123
Muenzer, H., Schroeter, E. H., Woehl, H., et al. 1989, A&A, 213, 431
Patsourakos, S., Vial, J. C., Gabriel, A. H., & Bellamine, N. 1999, ApJ, 522, 540
Priyal, M., Singh, J., Ravindra, B., et al. 2014, SoPh, 289, 137
Priyal, M., Singh, J., Ravindra, B., et al. 2023, ApJ, 944, 218
Raju, K. P. 2016, SoPh, 291, 3519
Raju, K. P. 2018, MNRAS, 478, 5056
Raju, K. P. 2020, ApJL, 899, L35
Raju, K. P., & Singh, J. 2002, SoPh, 207, 11
Raju, K. P., Singh, J., Ravindra, B., et al. 2023, ApJL, 959, L24
Reeves, E. M. 1976, SoPh, 46, 53
Rincon, F., & Rieutord, M. 2018, LRSP, 15, 6
Roudier, T., Švanda, M., Rieutord, M., et al. 2014, A&A, 567, A138
Sindhuja, G., Singh, J., & Ravindra, B. 2014, ApJ, 792, 22
Simon, G. W., & Leighton, R. B. 1964, ApJ, 140, 1120
Singh, J., & Bappu, M. K. V. 1981, SoPh, 71, 161
Singh, J., Priyal, M., & Ravindra, B. 2021, ApJ, 908, 210
Snodgrass, H. B., & Ulrich, R. K. 1990, ApJ, 351, 309
Sridharan, R. 2017-18IIA Annual Report
Sýkora, J. 1970, SoPh, 13, 292
Tian, H., Marsch, E., Tu, C. Y., Xia, L. D., & He, J. S. 2008, A&A, 482, 267
Wang, H. 1988, SoPh, 117, 343